

# Physiological Consequences of Abnormal Connectivity in a Developmental Epilepsy

Mouhsin M. Shafi, MD, PhD,<sup>1,2</sup> Marine Vernet, PhD,<sup>1</sup> Debby Klooster, MSc,<sup>3</sup>  
 Catherine J. Chu, MD,<sup>4</sup> Katica Boric, PhD,<sup>4</sup> Mollie E. Barnard, BA,<sup>5</sup>  
 Kelsey Romatoski, BA,<sup>2</sup> M. Brandon Westover, MD, PhD,<sup>4</sup>  
 Joanna A. Christodoulou, EdD,<sup>6</sup> John D. E. Gabrieli, PhD,<sup>7</sup>  
 Susan Whitfield-Gabrieli, PhD,<sup>7</sup> Alvaro Pascual-Leone, MD, PhD,<sup>1</sup> and  
 Bernard S. Chang, MD<sup>2</sup>

**Objective:** Many forms of epilepsy are associated with aberrant neuronal connections, but the relationship between such pathological connectivity and the underlying physiological predisposition to seizures is unclear. We sought to characterize the cortical excitability profile of a developmental form of epilepsy known to have structural and functional connectivity abnormalities.

**Methods:** We employed transcranial magnetic stimulation (TMS) with simultaneous electroencephalographic (EEG) recording in 8 patients with epilepsy from periventricular nodular heterotopia and matched healthy controls. We used connectivity imaging findings to guide TMS targeting and compared the evoked responses to single-pulse stimulation from different cortical regions.

**Results:** Heterotopia patients with active epilepsy demonstrated a relatively augmented late cortical response that was greater than that of matched controls. This abnormality was specific to cortical regions with connectivity to sub-cortical heterotopic gray matter. Topographic mapping of the late response differences showed distributed cortical networks that were not limited to the stimulation site, and source analysis in 1 subject revealed that the generator of abnormal TMS-evoked activity overlapped with the spike and seizure onset zone.

**Interpretation:** Our findings indicate that patients with epilepsy from gray matter heterotopia have altered cortical physiology consistent with hyperexcitability, and that this abnormality is specifically linked to the presence of aberrant connectivity. These results support the idea that TMS-EEG could be a useful biomarker in epilepsy in gray matter heterotopia, expand our understanding of circuit mechanisms of epileptogenesis, and have potential implications for therapeutic neuromodulation in similar epileptic conditions associated with deep lesions.

ANN NEUROL 2015;77:487–503

Epilepsy is among the most common, disabling, and costly neurological disorders in the world. In many forms of epilepsy, both acquired and developmental, aberrant connections involving cortical neurons appear to be pathogenically important.<sup>1–3</sup> Such circuitry has been associated in animal models with both local distur-

bances of cortical excitability as well as functional alterations in larger brain networks.<sup>4,5</sup> Unfortunately, our ability to investigate these physiological changes in patients with epilepsy is limited. Intracranial electrode recordings have shown signs of hyperexcitability within epileptogenic cortex as well as excessive synchrony

View this article online at [wileyonlinelibrary.com](http://wileyonlinelibrary.com). DOI: 10.1002/ana.24343

Received Sep 2, 2014, and in revised form Nov 26, 2014. Accepted for publication Dec 7, 2014.

Address correspondence to Dr Shafi, West/Baker 5, Beth Israel Deaconess Medical Center, 330 Brookline Ave, Boston, MA 02215. E-mail: [mshafi@bidmc.harvard.edu](mailto:mshafi@bidmc.harvard.edu)

From the <sup>1</sup>Berenson–Allen Center for Noninvasive Brain Stimulation, Department of Neurology, Beth Israel Deaconess Medical Center and Harvard Medical School, Boston, MA; <sup>2</sup>Comprehensive Epilepsy Center, Department of Neurology, Beth Israel Deaconess Medical Center and Harvard Medical School, Boston, MA; <sup>3</sup>Kempenhaeghe, Academic Center for Epileptology, Heeze, the Netherlands; <sup>4</sup>Department of Neurology, Massachusetts General Hospital and Harvard Medical School, Boston, MA; <sup>5</sup>Harvard School of Public Health, Boston, MA; <sup>6</sup>Department of Communication Sciences and Disorders, MGH Institute of Health Professions, Boston, MA; and <sup>7</sup>Department of Brain and Cognitive Sciences, Massachusetts Institute of Technology, Cambridge, MA

Additional Supporting Information may be found in the online version of this article.

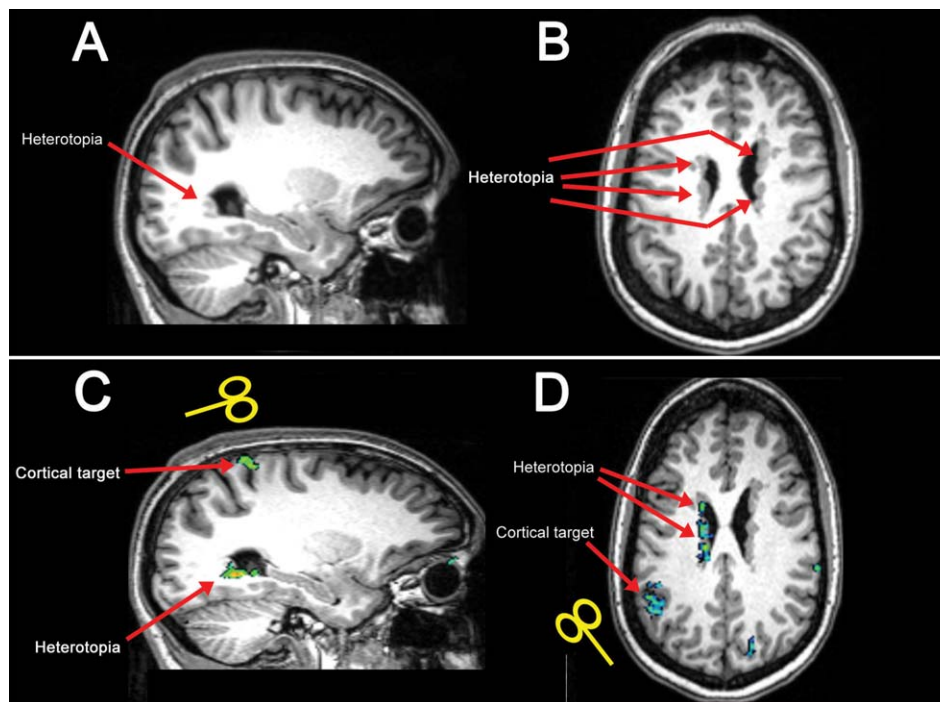


**FIGURE 1:** Anatomy and functional connectivity in patients with periventricular nodular heterotopia. T1-weighted magnetic resonance brain images show unilateral posterior gray matter heterotopia along the wall of the lateral ventricle in 1 patient, Subject 3 in Table 1 (sagittal image in A), and diffuse bilateral periventricular heterotopic nodules in another patient, Subject 7 (axial image in B), as indicated by red arrows. Blood oxygenation level–dependent images acquired in these patients reveal discrete regions of cerebral cortex that demonstrate aberrant functional connectivity with the heterotopic gray matter during the task-free resting state (green areas show significant functional activation in C and D); these regions were then chosen as cortical targets for transcranial magnetic stimulation in our experimental design.

between aberrantly connected regions of gray matter.<sup>2</sup> However, these studies require neurosurgical implantation and do not allow for significant experimental control or manipulation.

The unique developmental brain malformation of periventricular nodular heterotopia (PNH) offers an opportunity to study epileptogenic circuits and focal hyperexcitability in an anatomically well-characterized and often genetically determined disorder that leads to a seizure disorder only after an average latency of 20 years from birth.<sup>6–11</sup> PNH is a commonly encountered epileptic brain malformation, has a distinct radiological appearance that facilitates its initial diagnosis (Fig 1),<sup>12</sup> and generally presents with the clinical triad of epilepsy, reading disability, and normal intelligence.<sup>13,14</sup>

We previously demonstrated that the deep nodules of heterotopic gray matter in PNH are structurally and functionally connected to discrete foci of overlying cerebral cortex, and that the strength of this abnormal connectivity is higher among patients with longer durations of epilepsy.<sup>15</sup> In addition, we showed systematically that periventricular nodules can be metabolically coactivated with cortical regions during the performance of specific cognitive tasks, supporting the notion that these heterotopic nodules become integrated into functional cortical circuits.<sup>16</sup>

We hypothesized that epileptogenesis in this disorder is related specifically to focal hyperexcitability in cortical regions that have aberrant connectivity to the deep heterotopia, based on results from functional imaging, intracranial electroencephalography (EEG), and surgical outcome studies suggesting that particular areas of cortex might be critical to the generation of an epileptic state.<sup>7,9–11,17</sup> Proof of this hypothesis could potentially have broad mechanistic and therapeutic implications for similar forms of epilepsy, particularly those with a long latency to seizure onset, abnormal circuitry demonstrable by neuroimaging, or deep lesions inaccessible to noninvasive forms of antiepileptic brain modulation. A demonstration of cortical hyperexcitability that is spatially restricted to regions of abnormal functional connectivity would also expand our understanding of resting-state functional connectivity, as connectivity abnormalities have been identified in numerous neurological and psychiatric conditions but direct evidence that they have electrophysiologic significance is limited.<sup>18,19</sup>

In this study, we employed single-pulse transcranial magnetic stimulation (TMS) with simultaneous scalp EEG recording to investigate the cortical excitability profile of patients with PNH. TMS-EEG is a safe and noninvasive technique that has been used to probe cortical

activity in a variety of seizure disorder subtypes.<sup>20–22</sup> By using connectivity imaging findings to guide TMS targeting in a novel experimental design, we sought to determine the physiological implications of aberrant connectivity in this epileptic brain disorder.

## Subjects and Methods

### Subject Recruitment

Patients with epilepsy related to PNH were drawn from a research database of individuals with malformations of cortical development who had participated in prior studies, and whose initial connectivity imaging results were previously reported by us.<sup>15</sup> Patients with a neuroimaging-confirmed diagnosis of PNH based on the presence of at least 2 visible nodules of heterotopic gray matter adjacent to the lateral ventricle, each seen on >1 plane of sequence and on at least 2 consecutive images in 1 of those planes, were eligible to be enrolled. Those with prior brain surgery, inability to tolerate magnetic resonance imaging (MRI), or a specific MRI or TMS contraindication (including pregnancy) as set forth in standard institutional research protocols were excluded. Healthy control subjects, recruited from an existing research database and through advertisements, were matched to the PNH subjects by age (within 5 years), gender, and handedness. All control subjects were free of neurological symptoms and had normal anatomical brain MRI. All study participants provided written informed consent in accordance with research protocols approved by the institutional review boards of Beth Israel Deaconess Medical Center and the Massachusetts Institute of Technology.

### Brain Image Acquisition

Anatomical images and functional connectivity (fc) MRI images were acquired in all PNH subjects as previously described<sup>15</sup> on a Siemens 3T Magnetom Trio Tim system using a commercial 12-channel matrix head coil (Siemens Medical Solutions, Erlangen, Germany) and tetrahedron-shaped foam pads to minimize head movement. Sagittal localizer scans were aligned to a multisubject atlas to derive automatic slice prescription for consistent head position across subjects. High-resolution structural whole-brain images were acquired using a T1-weighted sequence with 128 slices per slab, a  $256 \times 256$  matrix, field of view (FOV) of 256 mm, slice thickness of 1.33mm with 0.63mm interslice gap, repetition time (TR) of 2,530 milliseconds, inversion time of 1,100 milliseconds, echo time (TE) of 3.39 milliseconds, and flip angle of  $7^\circ$ . Resting-state functional image acquisition was performed while subjects were asked to rest quietly (acquisition time = 6.4 minutes), using an echo-planar sequence sensitive to blood oxygenation level-dependent (BOLD) contrast with TR of 6,000 milliseconds, TE of 30 milliseconds, FOV of 256mm, voxel size of  $2.0 \times 2.0 \times 2.0$  mm, and flip angle of  $90^\circ$ .

### Functional Connectivity Analysis

fcMRI analyses were performed on the functional image data acquired during the task-free resting state with an in-house software toolbox, using methods previously described.<sup>23,24</sup> Func-

tional images were realigned and coregistered to anatomic images for each PNH subject, without normalization. Images were segmented, and BOLD signal was extracted. A band-pass filter ( $0.01 \text{ Hz} < f < 0.1 \text{ Hz}$ ) was applied, and Gaussian smoothing was performed (6 mm full width at half maximum). Several possible confounding sources of noise were identified and removed.<sup>25</sup> For each subject, multiple regions of interest (ROIs), which together encompassed the entire volume of heterotopic gray matter, were manually outlined in native space using MRI-CroN software<sup>26</sup> and served as seed regions for analysis. Color-coded functional connectivity maps were created for each seed ROI, showing correlations between the average BOLD signal time series of the ROI and that of every voxel in the brain, subject to a voxelwise statistical threshold of  $p < 0.001$  and cluster thresholding with an intensity cutoff as previously described.<sup>15</sup>

### Stimulation Target Creation

For each PNH subject, 2 regions of interest (the connected region and the nonconnected region) were determined based on the functional connectivity results. The connected region was manually outlined in MRICroN as a discrete region of cortex that demonstrated significant functional connectivity to a gray matter heterotopia ROI in the subject, based on the analyses described above (see Fig 1). The nonconnected region served as a control site and was manually outlined as a separate, discrete region of cortex that met the following criteria: (1) located within the same hemisphere as the connected region but at least 2.5cm away from it across the cortical surface (to avoid neighborhood stimulation effects during TMS), (2) contained the same volume of brain tissue as the connected region, and (3) demonstrated no evidence of significant functional connectivity (as identified by the methods described) to any gray matter heterotopia ROI in the subject. Targets for neuronavigated TMS were placed in the center of the connected and nonconnected regions. The exact Montreal Neurological Institute coordinates for each target in each PNH subject were then used for creation of the corresponding target in the matched healthy control subject. Targets were transferred directly into the TMS navigation software for visualization during the stimulation paradigm.

### TMS-EEG Experimental Setup

TMS was performed with a Nexstim eXimia stimulator with real-time MRI neuronavigation (NBS software v3.2.1; Nexstim, Helsinki, Finland) to ensure accurate stimulation of the targets defined by resting-state fcMRI. Monophasic pulses of TMS were administered via figure-of-eight coils (mean diameter = 59 mm, outer diameter = 70 mm), with the coil handle oriented posteriorly, perpendicular to the long axis of the target gyrus. EEG was recorded with a 60-channel TMS-compatible system (eXimia EEG, Nexstim), which utilizes a sample-and-hold circuit that holds the amplifier input constant from 100 microseconds prestimulus to 2 milliseconds poststimulus to avoid amplifier saturation by TMS.<sup>27</sup> EEG signals were referenced to an additional electrode on the forehead, filtered (0.1–500Hz), and sampled at 1,450 Hz with 16-bit resolution. Two extra sensors recorded electro-oculogram (EOG).

TABLE 1. Characteristics of Patients with Periventricular Nodular Heterotopia

Subject	Sex	Age, yr	Epilepsy Duration, yr	Seizure Frequency	Interval since Last Seizure, days	AEDs	Heterotopia, No./Laterality	Interictal EEG Findings	Resting Motor Threshold, Patient/Control <sup>a</sup>
1	M	42	34	~1 seizure/wk	7	Levetiracetam, lorazepam, oxcarbazepine, pregabalin	3/right, 3/left	Normal	80%/58%
2	M	23	15	~1 seizure/mo	21	Valproate, ezogabine, lacosamide	3/right	Right frontal and temporal spikes	62%/75%
3	F	20	6	~1 seizure/mo	41	Lamotrigine	2/right, ~3/left	Normal	92%/62%
4	F	30	5	~1 seizure/mo	14	Lamotrigine, levetiracetam	~7/right	Normal	75%/78%
5	M	22	5	~2 seizures/yr	216	Oxcarbazepine	1/right, ~5/left	Normal	67%/56%
6	F	28	6	No seizures in 7 years	2,484	None	2/right	Right frontotemporal slowing	57%/43%
7	F	34	10	No seizures in 10 years	3,726	Carbamazepine	~8/right, ~5/left	Normal	78%/37%
8	F	43	20	No seizures in 14 years	5,110	Lamotrigine	2/right, ~4/left	Right temporal spikes	81%/48%

Data in columns 3–7 were recorded at the time of transcranial magnetic stimulation. Resting motor thresholds are reported for each heterotopia subject and his or her matched healthy control.

<sup>a</sup>Percentage of maximum stimulator output.

AED = antiepileptic drug; EEG = electroencephalographic; F = female; M = male.

Electrode impedance was kept below 5 k $\Omega$  at all times. Resting motor threshold (RMT) was determined via surface electromyography (EMG) recorded using pregelled disposable Ag/AgCl electrodes, with the active electrode over the first dorsal interosseus (FDI) muscle, the reference electrode over the metacarpophalangeal joint, and the ground electrode over the wrist (Table 1).

### TMS-EEG Data Acquisition

Subjects were seated in a comfortable chair, and were asked to keep their eyes open, stare straight ahead, and maintain a relaxed state during stimulation. They were continually monitored for signs of drowsiness. All subjects wore earplugs to minimize risk of acoustic trauma.<sup>28</sup> At the beginning of each experiment, the RMT was determined by applying single pulses of TMS to motor cortex ipsilateral to the connected target site while the coil was placed at the optimal position for eliciting motor evoked potentials (MEPs) from the contralateral FDI muscle. The RMT was conventionally defined as the minimum stimulus intensity that elicited an MEP of at least 50  $\mu$ V in at least 5 of 10 trials.<sup>29</sup> Up to 80 single pulses of TMS at an intensity of 120% RMT were then administered every 5 to 6 seconds to the connected target and the nonconnected target, with simultaneous EEG recording. The order of stimulation of the target sites was randomized across subjects. In 1 subject (Subject 3 in Table 1), 120% RMT was greater than maximum stimulator output (MSO); in this subject, as well as in the matched control, single pulses of TMS were administered at 100% RMT (92% MSO).

### TMS-EEG Data Preprocessing

TMS-EEG data were processed offline using the EEGLab toolbox<sup>30</sup> and custom scripts running in MATLAB R2012b (MathWorks, Natick, MA). To minimize the effects of large-amplitude early TMS artifacts on subsequent preprocessing steps, and for visualization purposes, EEG data points during the period from 0 to 40 milliseconds after each stimulation pulse were replaced by interpolating between the potentials recorded at these 2 time points with a half-Gaussian curve with ends matched to the signal at 0 and 40 milliseconds. Because our analyses were restricted to the time period from 100 milliseconds after the pulse onward, this had no impact on our analyses. The TMS-EEG data were then downsampled to 1,000Hz, bandpass filtered between 1 and 100Hz, and notch filtered at 60Hz using a zero-phase finite impulse response filter. The continuous data were epoched from 1,000 milliseconds before to 2,000 milliseconds after each TMS pulse. Epochs were corrected with respect to the TMS-free prestimulus baseline period (−1,000 to −100 milliseconds). Each epoch was manually reviewed (by multiple researchers independently), and electrodes and epochs contaminated by significant muscle, movement, bad signal quality, or high-amplitude artifacts were removed. The data were then rereferenced to an average reference. Independent component analysis (ICA) was subsequently performed to identify and remove components reflecting residual muscle activity, eye movements, blink-related activity, and residual stimulation-related artifacts. Components were identified as

artifactual based on their topography, time courses, spectral characteristics, and association with EOG and/or stimulation pulse. After ICA cleaning, deleted electrodes were recomputed using a spherical spline interpolation, and the resulting data sets were low-pass filtered at 50Hz. The average (across epochs) TMS-evoked potential was then calculated at each electrode for each subject. To minimize the effects of any residual early TMS-evoked artifacts on our results, we focused our subsequent analysis on the time period from 100 to 1,000 milliseconds after each stimulation pulse.

### TMS-EEG Data Analysis

**GLOBAL MEAN FIELD POTENTIAL ANALYSIS.** For each subject, the global mean field potential (GMFP)<sup>31</sup> was calculated as a function of time. The GMFP has been used as a measure of the global brain response to TMS,<sup>32,33</sup> and is calculated using the equation:

$$GMFP(t) = \sqrt{\left[ \sum_i^K (V_i(t) - V_{mean}(t))^2 \right] / K}$$

where  $K$  is the number of electrodes,  $V_i(t)$  is the voltage measured at electrode  $i$  at time  $t$ , and  $V_{mean}(t)$  is the mean voltage across electrodes at time  $t$ .

To test our hypothesis that focal cortical hyperexcitability exists in patients with PNH and epilepsy, we segmented the TMS-evoked response into 4 time periods for analysis, based on prior studies demonstrating the normal response of primary motor cortex to single-pulse stimulation,<sup>32</sup> and studies reporting specific abnormalities of stimulation-evoked potentials (recorded by EMG and EEG) in patients with epilepsy.<sup>21,34,35</sup> The time periods were: (1) 100 to 225 milliseconds after the TMS pulse, corresponding to the period during which evoked activity is normally present (at least with stimulation of primary motor cortex); (2) 225 to 400 milliseconds after the TMS pulse, corresponding to the period that showed the greatest differences between epilepsy patients and healthy controls in prior TMS-EMG studies of primary motor cortex<sup>32</sup>; (3) 400 to 700 milliseconds after the TMS pulse; and (4) 700 to 1,000 milliseconds after the TMS pulse, to evaluate for abnormal delayed activity, which a previous TMS-EEG study suggested might be present in patients with epilepsy.<sup>21</sup>

For each subject, we calculated the area under the curve (AUC) of the baseline-corrected GMFP (AUC-GMFP) produced by stimulation of the connected target and the nonconnected target during each time period. The absolute magnitude of the evoked response can vary widely between individuals because of factors independent of cortical physiology (such as skull–cortex distance and individual brain anatomy), and as a function of brain region. To enable comparative assessments of the late elements of the evoked response independent of the absolute magnitude, we calculated the ratios of the delayed response to the early response. Specifically, we divided the AUC-GMFP during the 3 later time periods (225–400, 400–700, and 700–1000 milliseconds) by the AUC-GMFP

during the initial time period after TMS stimulation (100–225 milliseconds). We refer to the resulting values as the “normalized AUC-GMFP.” To obtain another measure of the evoked response, in the time periods showing significant differences on the normalized AUC-GMFP measures, we also identified the maximum amplitude of the largest peak in the GMFP produced by stimulation of the connected target and the non-connected target for each subject. The amplitudes of the largest peaks in these time periods were subsequently normalized by the amplitude of the largest peak in the 100- to 225-millisecond time period.

**GROUP COMPARISONS.** We evaluated differences in the TMS-evoked activity between all PNH subjects (regardless of epilepsy status) and their matched controls. For both the connected targets and the nonconnected targets, we assessed the significance of differences in the raw AUC-GMFP and in the normalized AUC-GMFP between all subjects with PNH and their matched controls using paired *t* tests. For the raw AUC-GMFP, as there were 4 time periods being compared for each stimulation site, differences were defined as significant at a probability value of  $<0.0125$  (Bonferroni-corrected  $p < 0.05$ ). For the normalized AUC-GMFP, as there were 3 time periods being compared, the significance threshold was set at a probability value of  $<0.0167$  (Bonferroni-corrected  $p < 0.05$ ). For the time periods that demonstrated significant group differences in AUC-GMFP measurements, we also evaluated group differences in the normalized amplitude of the maximum GMFP peaks, using paired *t* tests with a significance threshold of Bonferroni-corrected  $p < 0.05$ . Finally, to further evaluate the time course of the evoked response, we also determined the mean GMFP amplitudes (across subjects) over time, and conducted paired *t* tests at each time point. To correct for multiple comparisons, we used a false discovery rate (FDR) threshold of  $<0.05$ ,<sup>36</sup> as this has been suggested to be optimal for exploratory studies of evoked potential data.<sup>37</sup> Because our specific hypothesis predicted that abnormalities in cortical excitability would be most prominent in patients with active epilepsy, we repeated these analyses in the subset of 5 PNH subjects with at least 1 seizure in the past year (and their matched controls).

Similarly, to assess whether there were systemic differences in the evoked response produced by stimulation of the pathologically connected versus nonconnected target sites, we examined differences in the raw AUC-GMFP and normalized AUC-GMFP produced by stimulation of the connected versus nonconnected targets in PNH subjects using paired *t* tests, correcting for multiple comparisons done at each target. We also determined the mean GMFP amplitudes over time, as above, using paired *t* tests and a FDR threshold of  $<0.05$ . To ensure that any resulting differences were not simply due to intrinsic differences in excitability between the cortical regions represented among the connected and nonconnected targets, we determined these values with stimulation of the connected and nonconnected sites in the matched control subjects as well.

**SPATIAL DISTRIBUTION OF ABNORMAL EVOKED ACTIVITY.** The GMFP analysis provides a measure of the global response to TMS. We also examined the spatial topography of the abnormalities in evoked activity uncovered by GMFP analysis. For each electrode, the root mean square voltage (RMSV) during each time period was determined in each subject:

$$RMSV_{i,tp} = \sqrt{\sum_{t_{tp}}^{T_{tp}} V_i(t)^2}$$

where  $V_i(t)$  is the voltage measured at electrode *i* at time *t*,  $t_{tp}$  is the beginning of the time period (100, 225, 400, and 700 milliseconds), and  $T_{tp}$  represents the ending of the time period (225, 400, 700, and 1,000 milliseconds). As in the normalized AUC-GMFP analyses, the single-electrode RMSV during the later time periods (225–400, 400–700, and 700–1,000 milliseconds) was normalized by dividing by the RMSV during the initial time period (100–225 milliseconds), and the resulting normalized RMSV was subsequently log transformed for variance stabilization and to facilitate graphical representation of changes in the relative amplitude of evoked activity.

To isolate the regions that showed differential delayed-activity between PNH subjects with active epilepsy and their matched controls, the log-transformed normalized RMSVs from the healthy controls were subtracted from the values obtained from stimulation of the same site in the corresponding PNH subjects. A positive result indicates that the normalized RMSV was greater in the PNH subject than in the matched control subject, whereas a negative result indicates the converse.

**ANALYSIS OF LOCAL EVOKED ACTIVITY.** To further evaluate whether abnormalities in evoked activity were due solely to changes in local (vs distributed) activity, we examined the TMS-evoked responses in the region of stimulation. For each subject, the neighborhood of electrodes immediately surrounding the site of stimulation was defined as the ROI. For each time point, the mean of the absolute value of the voltages across electrodes (in this ROI) was determined (referred to as  $V_I$ ):

$$V_I(t) = \sum_i^{K_n} |V_i(t)| / K_n$$

where  $V_i(t)$  is the voltage measured at electrode *i* at time *t* and  $K_n$  is the set of neighboring electrodes.

As in the AUC-GMFP analysis, the AUC of the mean absolute local voltage (AUC-local) was determined for each time period (100–225, 225–400, 400–700, and 700–1,000 milliseconds), and the AUC-local during the later 3 time periods was normalized by dividing by the AUC-local during the initial time period. Significant differences between PNH subjects with active epilepsy and their matched healthy controls were assessed via paired *t* tests, adjusted for multiple comparisons.

**ELECTRICAL SOURCE IMAGING OF EVOKED ACTIVITY.** One PNH subject (Subject 2 in Table 1) had interictal epileptiform discharges and ictal recordings available on conventional

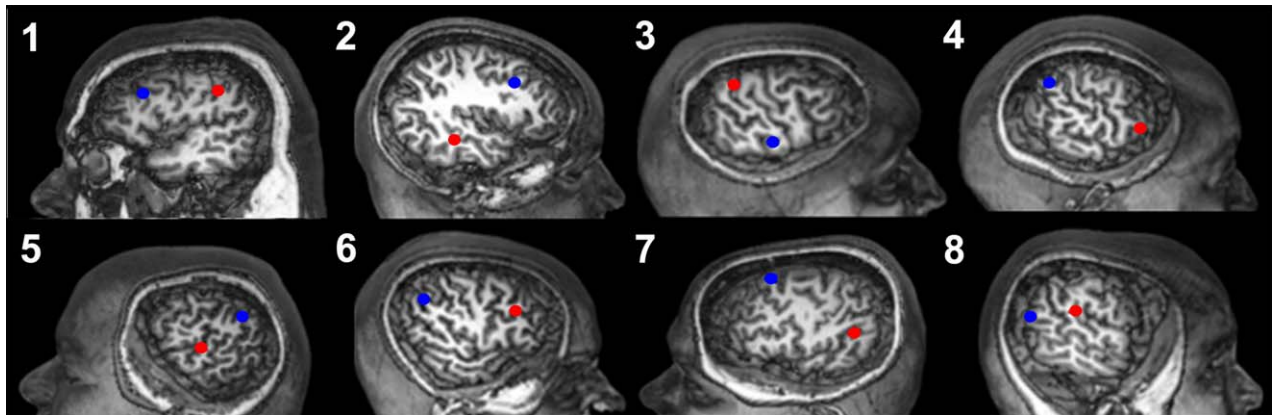


**FIGURE 2:** Connectivity-derived targets for cortical stimulation in patients with periventricular nodular heterotopia. Cortical regions that demonstrate significant resting-state functional connectivity to periventricular gray matter nodules in 8 patients with heterotopia, labeled according to subject number as listed in Table 1 and shown on surface brain magnetic resonance renderings, were identified. Connected targets (red) for neuronavigation-guided transcranial magnetic stimulation (TMS) were then placed within these regions in each case. Nonconnected cortical targets (blue), in regions without such connectivity, were also identified within the same hemisphere for each subject. Each control subject had neuronavigation-guided TMS of the same targets as his or her matched heterotopia subject.

scalp EEG (with 19 channels and a 10–20 montage). For this subject, we investigated whether abnormal TMS-evoked EEG activity had generator sources that spatially coincided with the known epileptogenic zone by comparing the electrical source analysis of these TMS-EEG peaks with that of the 2 most prominent available interictal discharges and the 2 available ictal onsets.

Source analysis of EEG data was performed using minimum norm estimate (MNE) software<sup>38,39</sup> with anatomical surfaces reconstructed using the FreeSurfer package.<sup>40</sup> MNE provides a distributed source estimate of cortical currents incorporating constraints from a subject's MRI, transforming the data to brain space without requiring heuristic choices or strong assumptions about the sources. Electrode location for this subject was not available (as an interpretable digitized file); thus, to find the electrode location, a file from an alternate patient with similar approximate head size was used. The subject's cortical surface was reconstructed from T1-weighted magnetization-prepared rapid acquisition gradient-echo data.<sup>40</sup> Electrode coordinates were aligned using the nasion and auricular points as fiducial markers. Head modeling utilized a 3-layer boundary element method (BEM) model that was generated using the reconstructed cortical surface and fast low-angle shot MRI data, composed of the scalp, skull, and brain with electrical conductivities of 0.33, 0.0042, and 0.33 S/m, respectively.<sup>38</sup> A 3-dimensional grid with 5 mm spacing was used to form the solution space. The forward solution was calculated by using the BEM. The inverse operator was computed from the forward solution with a loose orientation constraint of 0.6 to eliminate implausible sources and 2  $\mu$ V as the estimate of EEG noise. The resulting source data were thresholded to identify the region of maximal activity.

## Results

### Study Population

Eight patients with PNH were recruited (see Table 1), along with 8 age-, gender-, and handedness-matched

healthy control individuals. All PNH subjects had a history of at least 1 seizure in their lifetime; 5 (62%) had active epilepsy, with at least 1 seizure in the year prior to the TMS study visit. Seizure frequencies in these 5 subjects ranged from approximately 1 seizure per week to approximately 1 seizure every 6 months; interictal epileptiform discharges (IEDs) on EEG were present in 1 of these 5. The remaining 3 PNH subjects (38%) had well-controlled epilepsy, with no seizures in the preceding 5 years; 1 of these 3 had IEDs on EEG. All PNH subjects had at least 2 heterotopic gray matter nodules; 5 (62%) had bilateral nodules.

### Stimulation Targets

A target site functionally connected to a region of periventricular heterotopic gray matter (connected target) and another target site within the same hemisphere without abnormal functional connectivity (nonconnected target) were defined for each PNH subject as described in Subjects and Methods. The targets were right hemispheric in 5 subjects (62%) and left hemispheric in 3. The connected targets were located in the frontal (25%), temporal (25%), and parietal (50%) lobes (Fig 2). The nonconnected targets were located in the frontal (50%), parietal (38%), and occipital (12%) lobes.

### TMS-Evoked Potentials and GMFP Analyses

**TMS-EVOKED POTENTIALS.** In both PNH subjects and matched controls, TMS evoked a time-locked response characterized by recurrent waves of activity that evolved in amplitude and spatial distribution, lasting several hundred milliseconds (eg, Fig 3A–E). The precise pattern of activity varied as a function of the stimulation

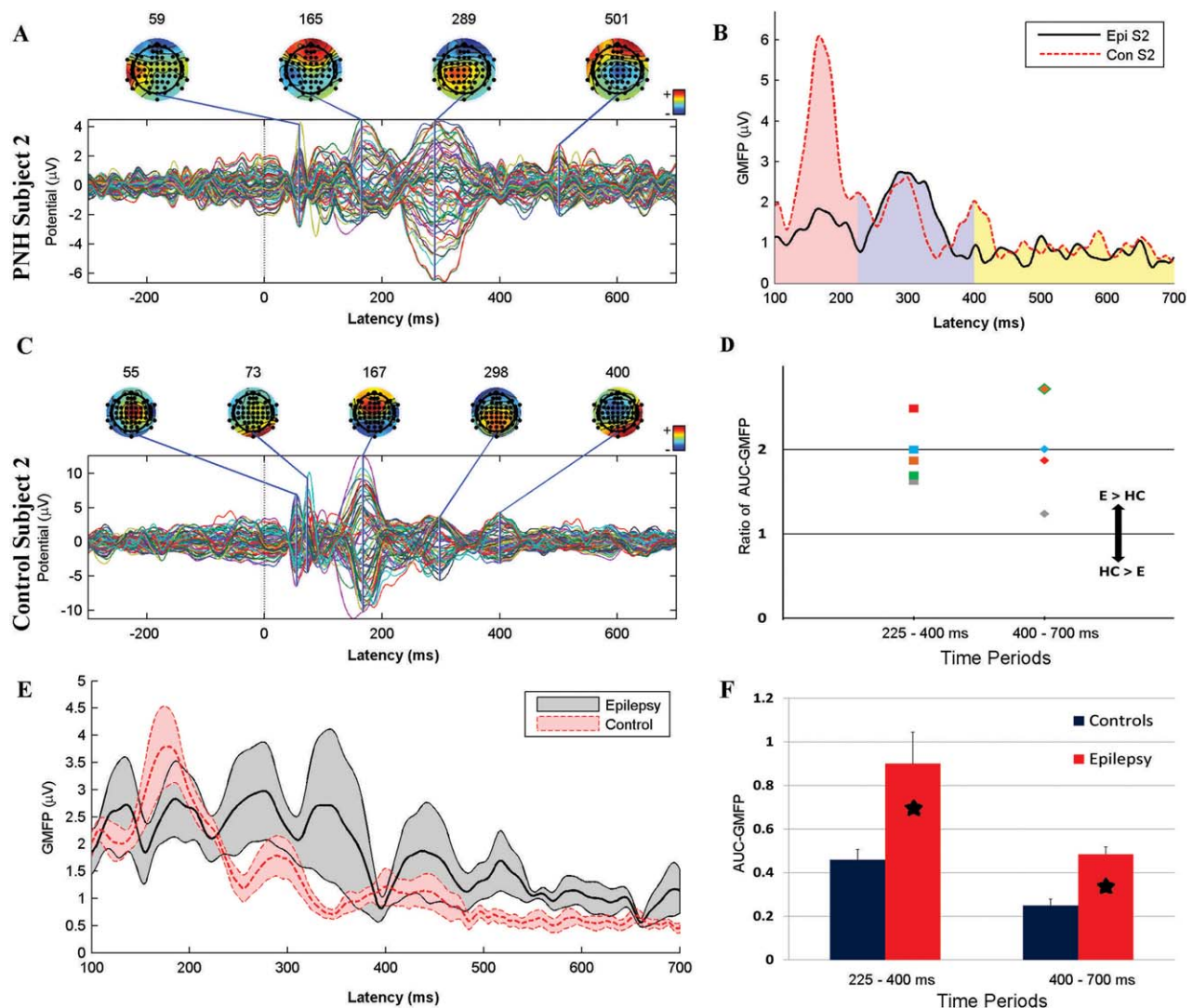


**FIGURE 3:** Augmented late transcranial magnetic stimulation (TMS)-evoked cortical responses in patients with periventricular nodular heterotopia (PNH) and active epilepsy. (A) The TMS-evoked response produced by stimulation of the connected target site in Subject 2. Note the relatively large evoked potential at 289 milliseconds as compared to earlier potentials. (B) The global mean field potential (GMFP) between 100 and 700 milliseconds after stimulation of the connected target in a PNH patient, Subject 2 (Epi; *solid black line*), and his matched control (Con; *dashed red line*). The pink region corresponds to the first time period (100–225 milliseconds after the pulse), the blue to the second (225–400 milliseconds), and the yellow to the third (400–700 milliseconds). (C) The TMS-evoked response produced by stimulation of the same site (as in A) in the matched control for Subject 2. Note that the potential at 167 milliseconds is substantially larger than later potentials. (D) The ratio of the normalized area under the curve (AUC) of the GMFP after stimulation of the connected target for each of the 5 PNH subjects with active epilepsy to the equivalent measure in their matched healthy controls, during the 225- to 400-millisecond and 400- to 700-millisecond time periods. A ratio  $>1$  indicates an augmented late cortical response in the epilepsy patient (E) as compared to the healthy control (HC). (E) The mean GMFP over time, across subjects, evoked by stimulation of the connected target site for the 5 PNH subjects with active epilepsy (*thick black line*) and their matched controls (*thick dashed red line*). The gray and red bands indicate  $\pm$ standard error of the mean. (F) The normalized AUC-GMFP averaged across all PNH subjects with active epilepsy and their matched healthy controls during the same 2 time periods as in D. Asterisks indicate significant differences (Bonferroni-corrected  $p < 0.05$ ). Note that the raw evoked potentials in A and C are not plotted on a uniform scale.

site, and thus varied between the connected and nonconnected targets, and between subject pairs (eg, note the different patterns evoked by stimulation of a different site in another PNH subject and healthy control pair in Fig 4; see also Supplementary Fig for the raw GMFPs provoked by stimulation in all subjects).

Despite the variability in the TMS-evoked potentials between stimulation targets within subjects and between subject pairs, some prominent features were apparent. In healthy controls, stimulation resulted in an evoked response that was maximal within the first 225 milliseconds and then attenuated (see Figs 3C, E

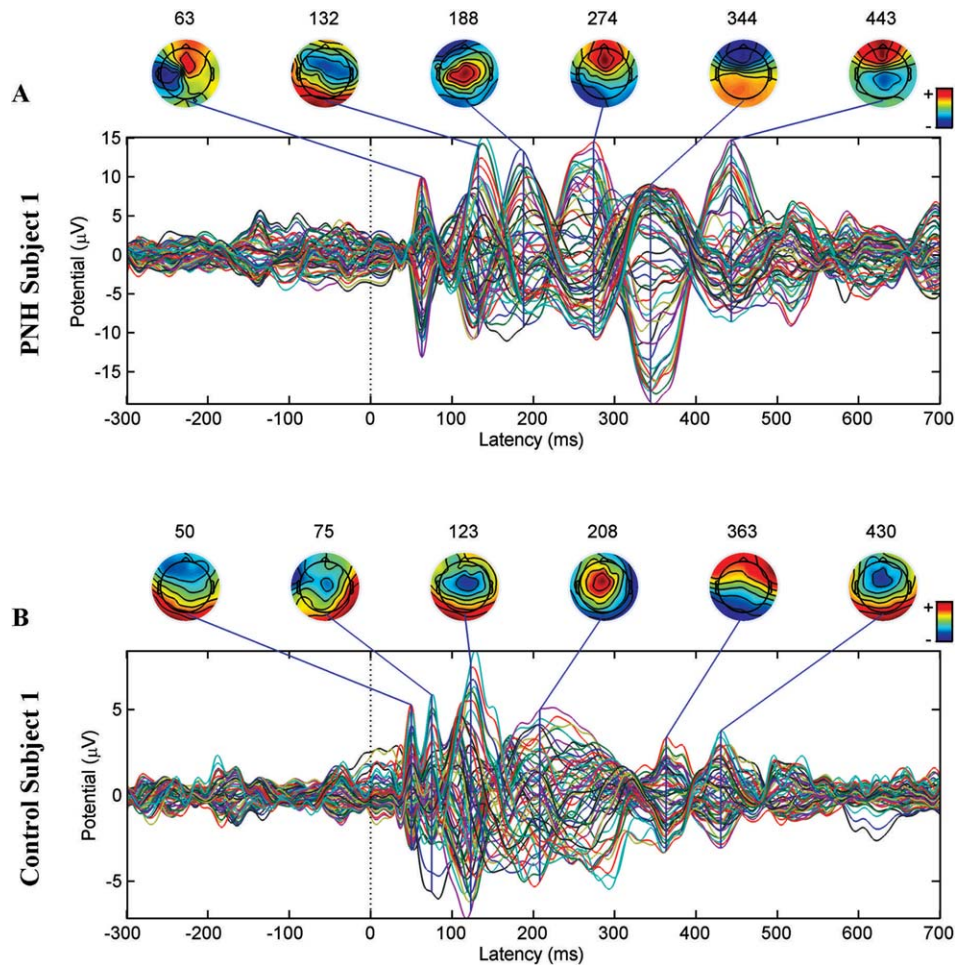


**FIGURE 4:** Persistent transcranial magnetic stimulation (TMS)-evoked activity in a patient with periventricular nodular heterotopia (PNH) and active epilepsy, but with a normal interictal electroencephalogram (EEG). (A) The TMS-evoked response produced by stimulation of the connected target site in Subject 1. (B) The TMS-evoked response produced by stimulation of the same site in the matched healthy control subject. The later peaks (>225 milliseconds) in the PNH subject are of the same magnitude as or larger than earlier peaks, whereas the later peaks are smaller than the earlier peaks in the matched healthy control subject. Notably, Subject 1 had entirely normal interictal findings on prolonged continuous EEG monitoring. Note that the evoked potentials are not plotted on a uniform scale.

and 4B). In contrast, in PNH subjects with active epilepsy, the response evoked by stimulation of the abnormally connected target was sustained (see Fig 4A) or even increased (see Fig 3A) at later time points. This was true even for those subjects with normal interictal EEG findings, notably including 1 subject (Subject 1; see Fig 4A) who had no IEDs recorded during 11 days of continuous EEG monitoring (that did capture 3 electrographic seizures). Topographic mapping of these delayed responses demonstrated evolving spatial distributions of evoked activity throughout the later time periods.

**GMFP ANALYSIS.** PNH Subjects Compared to Healthy Controls. There was a significant difference (Bonferroni-corrected  $p < 0.05$ ) between PNH subjects

with active epilepsy and their matched healthy controls in the normalized AUC-GMFP with stimulation of the connected target (see Fig 3B, D, F; Supplementary Fig). Specifically, the normalized AUC-GMFP produced by stimulation of the connected target was significantly greater in those with active epilepsy for the 225- to 400-millisecond and the 400- to 700-millisecond periods; there was no significant difference in the 700- to 1,000-millisecond period. In contrast, there were no significant differences in the normalized AUC-GMFP with stimulation of the nonconnected target.

When comparing all PNH subjects (regardless of epilepsy status) with their matched controls, there were no significant differences (Bonferroni-corrected  $p > 0.05$ ) in the normalized AUC-GMFP after stimulation of either the connected target or the nonconnected target in

**TABLE 2. Maximum Peak Amplitudes and Ratios in the Global Mean Field Potential after Transcranial Magnetic Stimulation of Cortical Targets with Aberrant Connectivity**

Subject	Period 1 Peak, 100–225 ms, $\mu\text{V}$	Period 2 Peak, 225–400 ms, $\mu\text{V}$	Period 2 Peak/Period 1 Peak	Period 3 Peak, 400–700 ms, $\mu\text{V}$	Period 3 Peak/Period 1 Peak
1	6.700	8.969	1.339	5.950	0.888
C1	3.560	2.305	0.647	1.712	0.481
2	1.836	2.742	1.493	1.160	0.632
C2	6.096	2.621	0.430	2.016	0.331
3	3.418	1.526	0.446	1.542	0.451
C3	2.668	0.885	0.332	0.5422	0.203
4	1.962	1.933	0.985	1.088	0.555
C4	3.845	1.115	0.290	0.9312	0.242
5	3.236	2.946	0.910	1.952	0.603
C5	5.831	2.854	0.489	2.514	0.431

Periventricular nodular heterotopia (PNH) subjects with active epilepsy are numbered as in Table 1. C1–C5 represent the matched healthy controls for Subjects 1–5, respectively. Columns 2, 3, and 5 show the maximum amplitudes of the largest peak evoked by stimulation of the connected target in each of the 3 time periods for the PNH subjects and their matched controls. Columns 4 and 6 show the ratios of the maximum amplitudes during the late versus early time periods.

any time period. There were also no significant differences between PNH subjects (or the subset with active epilepsy) and matched healthy controls in the raw AUC-GMFP for any time period with stimulation of either target.

There was a significant difference between PNH subjects with active epilepsy and their matched controls in the normalized amplitude of the largest peaks in the GMFP evoked by stimulation of the connected target during the 225- to 400-millisecond and 400- to 700-millisecond time periods (Table 2; Bonferroni-adjusted  $p < 0.05$ ), again consistent with a relative increase in late activity with stimulation of the connected target. There were no significant differences between these subjects and their matched controls in normalized maximal peak amplitudes with stimulation of the nonconnected site, or between all PNH subjects and their matched controls with stimulation of either site.

There were no significant differences in the GMFP amplitudes at any individual time point with stimulation of either target, although the pattern of the activity evoked by stimulation of the connected target appeared different between PNH subjects with active epilepsy and their matched controls (see Fig 3E).

**GMFP ANALYSIS.** Connected Targets Compared to Nonconnected Targets. There were differences in evoked activity with stimulation of the connected versus

nonconnected target site in PNH subjects and their matched controls (Fig 5). There was a significant difference (Bonferroni-corrected  $p < 0.05$ ) in the normalized AUC-GMFP between stimulation of the connected versus nonconnected target sites in all PNH subjects. Specifically, the normalized AUC-GMFP was significantly greater with stimulation of the connected target for the 225- to 400-millisecond and the 400- to 700-millisecond time periods; there was no significant difference for the 700- to 1,000-millisecond time period. These differences were not simply due to inherent differences between the cortical regions represented by the connected and nonconnected targets, as there were no significant differences in the normalized AUC-GMFP between stimulation of the 2 sites in the matched healthy controls ( $p > 0.05$ ). A similar effect was seen in the subset of patients with active epilepsy, although the difference only reached significance (Bonferroni-corrected  $p < 0.05$ ) for the 225- to 400-millisecond time period in this smaller subgroup.

There was no significant difference in the raw AUC-GMFP evoked by stimulation of the connected versus nonconnected target in any of the subject groups. There were no significant differences in the normalized amplitudes of the largest peaks with stimulation of the connected versus nonconnected target in any group, except for a significant increase ( $p < 0.05$ ) in the normalized maximum peak in the 400- to 700-millisecond time range with stimulation of the connected versus

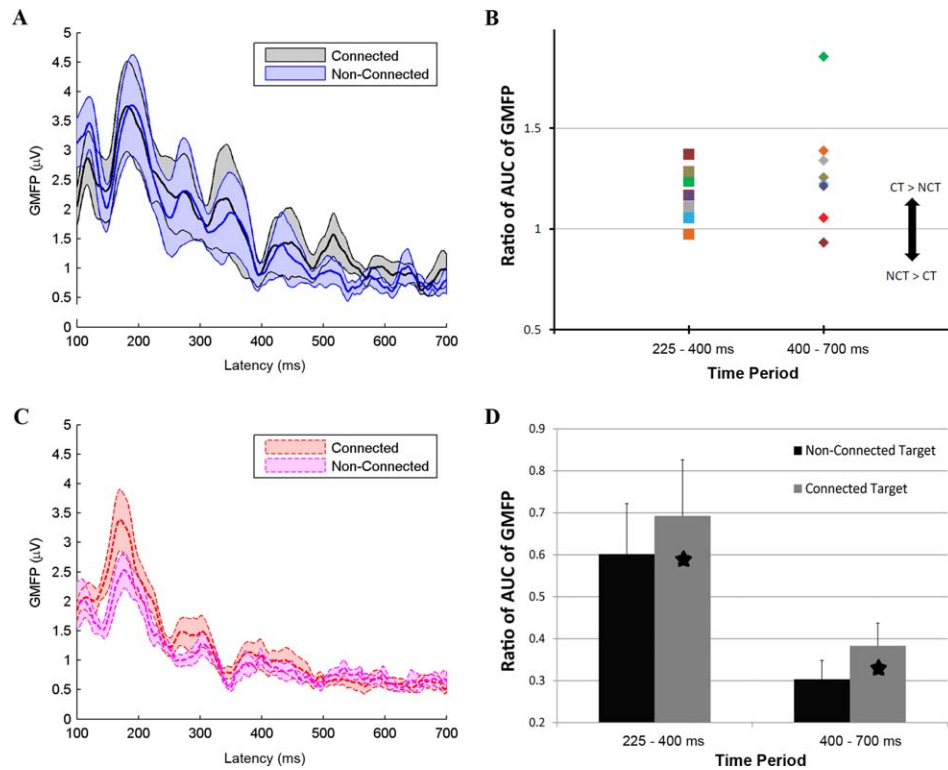


**FIGURE 5: Augmented late transcranial magnetic stimulation–evoked cortical responses specific to stimulation of cortical regions with aberrant functional connectivity.** (A) The mean global mean field potential (GMFP) over time, across all periventricular nodular heterotopia (PNH) subjects, evoked by stimulation of the connected target site (*thick black line*) and the nonconnected target site (*thick blue line*). The gray and blue bands indicate  $\pm$ standard error of the mean. (B) The ratio of the normalized area under the curve (AUC) of the GMFP after stimulation of the connected target to the equivalent measure after stimulation of the nonconnected target in each of the PNH subjects during the 225- to 400-millisecond and 400- to 700-millisecond time periods. A ratio  $>1$  indicates an augmented late cortical response after stimulation of the connected target (CT) as compared to the nonconnected target (NCT). (C) The mean GMFP over time, across all healthy control subjects, evoked by stimulation of the connected target site (*thick dashed red line*) and the nonconnected target site (*thick dashed purple line*). The red and purple bands indicate  $\pm$ standard error of the mean. (D) The normalized AUC-GMFP averaged across all connected and nonconnected targets in the PNH subjects for the same 2 time periods as in B. Asterisks indicate significant differences (Bonferroni-corrected  $p < 0.05$ ).

nonconnected target in the PNH subjects with active epilepsy. There were no significant differences in the magnitude of the GMFP with stimulation of the connected versus nonconnected target at any time point in either the PNH subjects or the matched controls ( $FDR > 0.05$ ).

### **Spatial Distribution of Abnormal Evoked Activity**

We evaluated the spatial distribution of the abnormally increased delayed activity produced by stimulation of the connected targets in PNH subjects with active epilepsy relative to their matched controls. Topographic plots displaying the differences in the log-transformed RMSV (see Subjects and Methods) with stimulation of the connected targets are shown (Fig 6). Whereas in some subjects increased evoked activity was present at or immediately adjacent to the site of stimulation (eg, subject pair 3), in others the focus of increased activity was

spatially remote from the stimulation site (eg, subject pair 1, left column). Notably, regions with increased activity were often located in the contralateral hemisphere. Furthermore, multiple discrete regions of abnormally increased activity were often present (eg, subject pairs 1, 4, and 5). There were no significant differences (Bonferroni-corrected  $p > 0.05$ ) between PNH subjects with active epilepsy and their matched controls in the measure of local evoked activity (see Subjects and Methods) produced by stimulation of the connected targets for any time period.

### **Electrical Source Imaging**

Subject 2 was the only PNH patient who had an epileptogenic zone determinable on available scalp EEG recordings. To identify whether the late TMS-EEG peaks (at 289 and 501 milliseconds after stimulation of the connected target; see Fig 3A) had generator sources that

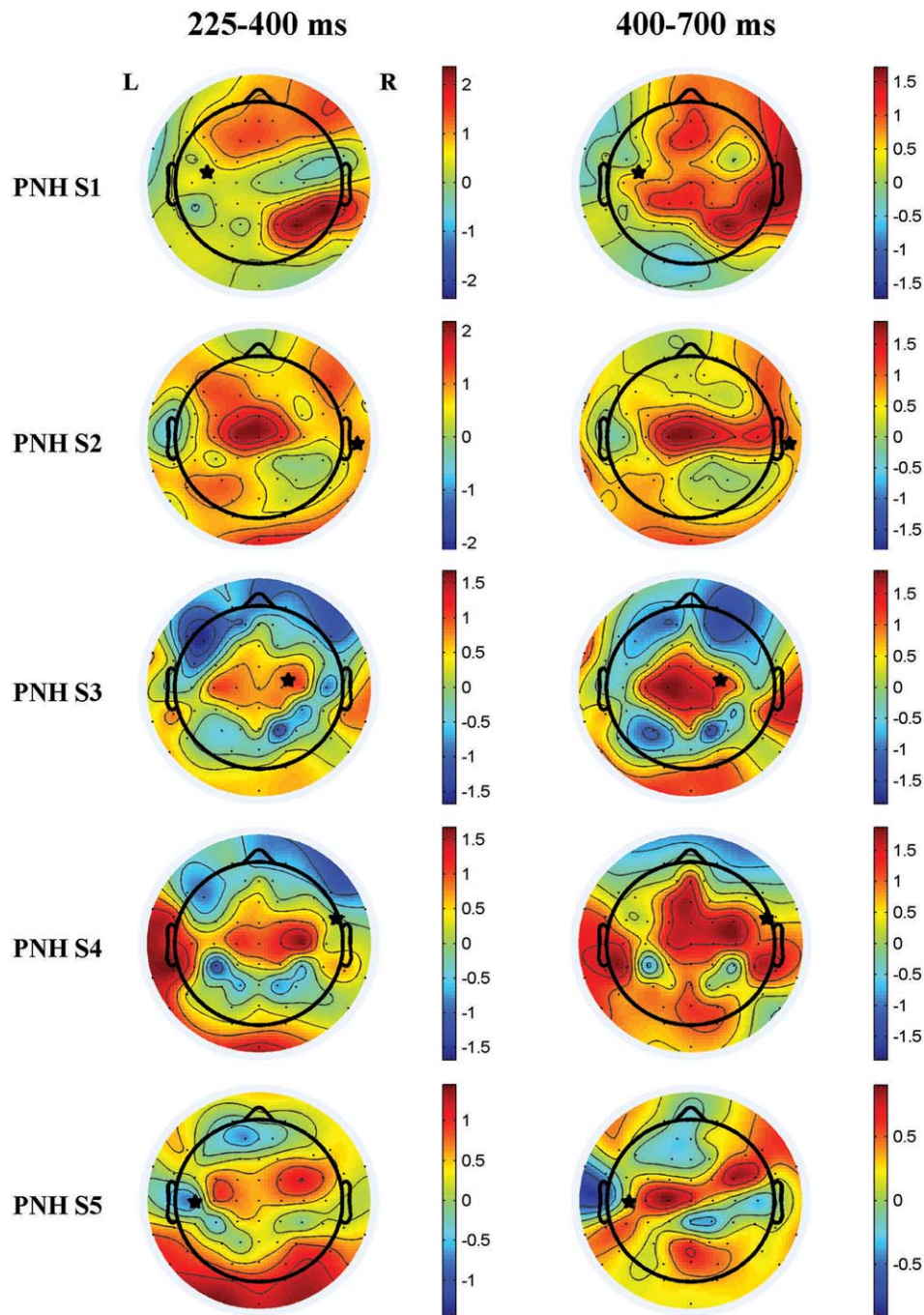


**FIGURE 6:** Topography of differences in transcranial magnetic stimulation–evoked activity between patients with periventricular nodular heterotopia (PNH) and active epilepsy and matched healthy controls. The plots show the differences between PNH patients with active epilepsy (Subjects 1–5) and their matched healthy controls in the log-transformed normalized root mean square voltage at each electrode evoked by stimulation of the connected target. Warm colors indicate regions where the evoked activity was greater in the patient; cool colors indicate that the evoked activity was greater in the control. Asterisks indicate the site of stimulation (the connected target site). The left side of each image represents the left side of the brain. L = left; R = right.

were spatially coincident with the spike and seizure focus, we performed source analysis on the 2 TMS-EEG peaks (Fig 7A, B), the 2 most prominent available interictal discharges (see Fig 7C, E), and the 2 available periods of ictal onset on the subject’s scalp EEG recordings (see Fig 7D, F) using the MNE method as described.

In all 6 instances, source imaging results converged on a focus in the right frontal lobe. This region was not near the connected target of stimulation (as seen in Fig 2), but instead overlapped with a cortical region that demonstrated functional connectivity to an underlying gray matter heterotopic nodule in the right hemisphere.

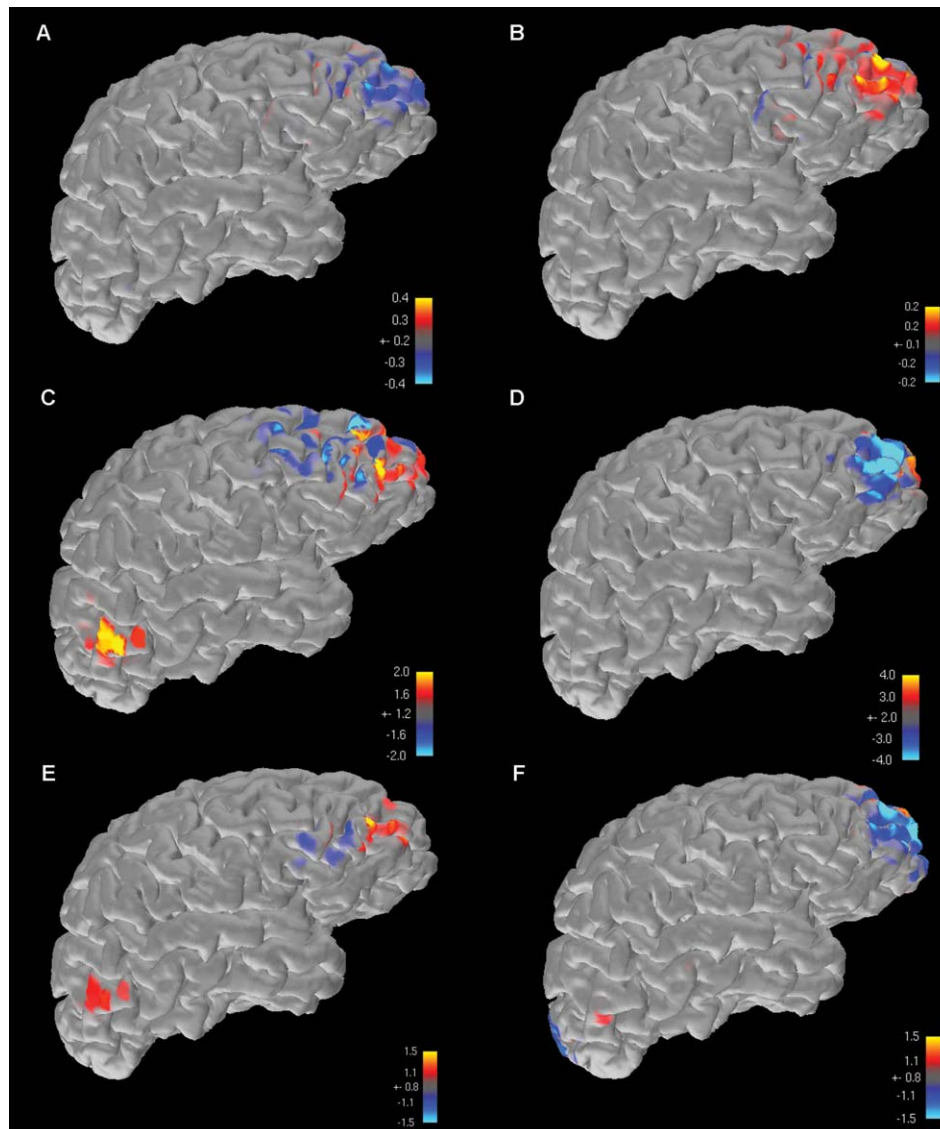


**FIGURE 7:** Source analysis results of transcranial magnetic stimulation (TMS)-evoked activity, interictal epileptiform activity, and ictal onset activity. In Subject 2, the only periventricular nodular heterotopia patient in this study with an identifiable epileptogenic zone on scalp electroencephalogram (EEG), electrical source imaging was performed on the 2 late TMS-EEG peaks seen after stimulation of the connected target (A, B), 2 prominent interictal epileptiform discharges seen on conventional scalp EEG recording (C, E), and ictal onsets of the 2 recorded seizures available on scalp EEG (D, F). Warm colors represent positive maxima, whereas cool colors represent negative maxima. In all instances, results converge on an area of the right frontal lobe that was not the site of stimulation, but overlapped with a cortical region that demonstrated functional connectivity to an underlying heterotopic nodule.

## Discussion

Here we demonstrate that patients with epilepsy associated with the developmental brain malformation of PNH show evidence of altered cortical physiology, and that these changes detected by TMS-EEG appear to be limited to cortical regions with aberrant functional connectivity to deep regions of gray matter heterotopia. The nature of these abnormalities, which are specifically characterized by a relatively augmented late response that is widely distributed beyond the site of local stimulation, is most consistent with cortical hyperexcitability, and

supports the hypothesis that aberrant gray matter connectivity in this disorder leads to epileptogenesis through alterations in cortical neurophysiology. In the 1 subject who had an epileptogenic zone determinable by scalp EEG, the generator source of the abnormal TMS-evoked activity was spatially coincident with the spike and seizure onset zone. The findings from our small sample support the potential utility of TMS-EEG as a novel and informative biomarker in certain forms of epilepsy, expand our mechanistic understanding of network changes as the pathological basis for seizures in gray

matter heterotopia, provide support for the use of resting-state functional connectivity imaging in neuropsychiatric disorders, and raise the possibility of noninvasive therapeutic neuromodulation in similar seizure disorders associated with deep lesions.

### **TMS-EEG and Cortical Excitability in Epilepsy**

TMS has been increasingly used in recent years as a safe and noninvasive technique of probing cortical physiology in a number of neurological and psychiatric disorders.<sup>41,42</sup> TMS has typically been coupled with the electromyographic recording of MEPs during stimulation of the motor cortex, and numerous TMS-MEP studies in epilepsy have shown alterations in motor cortex excitability, including in patients with both focal<sup>43</sup> and generalized<sup>44</sup> syndromes. The use of TMS with simultaneous scalp EEG, although technically challenging, allows for the determination of physiological responsiveness over more widespread regions of nonmotor cortex. The TMS-evoked cortical response as recorded on EEG consists of a highly reproducible sequence of early waveforms that provide information on the excitability and oscillatory properties of the stimulated cortical target; these are thought to reflect fluctuations of excitatory and inhibitory postsynaptic activity, particularly as modulated by  $\gamma$ -aminobutyric acidergic neurotransmission.<sup>45,46</sup>

A small number of TMS-EEG studies have shown that hyperexcitability and late oscillatory activity can be seen from nonmotor regions of cortex in epilepsy patients,<sup>21,22</sup> suggesting augmented excitatory and/or diminished inhibitory local activity and a prolonged reverberation of cortical activity as contributors to the epileptic state. Our data confirm and extend these prior results. The analysis of TMS-evoked potentials allows us to determine cortical excitability “on demand,” rather than wait for spontaneous epileptiform activity. Eighty percent of our patients with active epilepsy had normal interictal EEG recordings, yet there were robust abnormalities in TMS-evoked responses in this group, indicating that TMS-EEG adds information above and beyond scalp EEG studies, even long-term recordings (as demonstrated in Subject 1, who had no IEDs during 11 days of continuous recording). In our study, demonstration of the relative augmentation of late (>225 milliseconds poststimulation) responses, which takes the form of persistent oscillatory activity with widespread and shifting topography, appears to be most consistent with a reverberation of epileptic activity through large-scale neural circuits.

### **Aberrant Connectivity and Network Changes in Epileptogenesis**

PNH is an uncommon disorder, estimated to be responsible for about 2% of medically refractory epilepsy.<sup>6</sup>

However, its unique characteristics make it well suited as a model for circuit epileptogenesis, due to its well-defined and often genetically determined anatomical findings, its long latency to epilepsy onset, and its association with normal intelligence (which allows for cooperation with imaging, stimulation, and behavioral testing in the absence of confounding cognitive impairment). A longstanding question in PNH and related cortical malformations is how the onset of epilepsy can be delayed for years or decades after birth given the striking abnormalities of cerebral architecture that arise from defects in neuronal migration or other steps in fetal brain development. This study links the known alterations in structural and functional connectivity in PNH<sup>15</sup> to specific changes in cortical physiology that may underlie the process of epileptogenesis. Whereas some patients with PNH have bilateral widespread nodules, others have more anatomically limited regions of heterotopia. Our finding of a significant difference in the late TMS-evoked response between cortical regions with demonstrated aberrant connectivity and control regions without such connectivity, within the same hemispheres of the same individuals, demonstrates that hyperexcitability in PNH is not simply a diffuse phenomenon but is specifically linked to the presence of corticoheterotopic circuitry. In the 1 subject with an identifiable epileptogenic zone by scalp EEG, source modeling results for interictal spikes, ictal epileptiform activity, and abnormal late TMS-EEG activity all converged on a right frontal focus, where a region of aberrant functional connectivity to underlying heterotopia was seen.

A number of very common epileptic conditions are now thought to be associated with the gradual development of aberrant cortical connectivity over time,<sup>3</sup> including epilepsy after head injury,<sup>47</sup> poststroke epilepsy,<sup>48</sup> and epilepsy of medial temporal lobe onset.<sup>49</sup> Similar studies in these disorders could identify whether pathologic circuit mechanisms analogous to those in gray matter heterotopia also lead to seizures in these conditions.

### **Neurophysiological Markers of Aberrant Resting-State Functional Connectivity**

A fundamental concept underlying resting-state fMRI studies is that regions with coherent BOLD fluctuations interact in a neurophysiologically meaningful manner, and that alterations in the “normal” pattern of resting-state connectivity have pathologic significance.<sup>50</sup> However, direct physiologic evidence for this concept is lacking. In this study, regions with abnormal resting-state connectivity were shown to have abnormal TMS-evoked EEG activity that correlated with disease state, whereas regions without such connectivity did not show such

abnormalities. These results provide critical evidence that alterations in resting-state functional connectivity, which have been widely reported in a number of different conditions,<sup>18</sup> can be directly linked to pathologically important neurophysiological changes (at least in this epilepsy syndrome), and that TMS-EEG metrics can be used to assess the physiological significance of abnormal connectivity directly.

### **Potential for Noninvasive Therapeutic Modulation Based on Connectivity Imaging**

Low-frequency repetitive TMS (rTMS) is known to downmodulate cortical excitability at the stimulation target, and in some clinical trials for epilepsy, has significantly reduced seizure frequency, particularly when ictal foci are neocortical and associated with visible anatomical lesions (and thus easily accessible for TMS targeting).<sup>51,52</sup> Deep lesions, such as periventricular nodules or even mesial temporal sclerosis, however, cannot be selectively modulated by conventional TMS coils.<sup>53</sup> Our results suggest that hyperexcitable cortical “partner” regions of deep lesions can be identified through structural and functional connectivity imaging, and could be accessible to neuromodulatory techniques that are successful at treating neocortical foci. This same principle underlies the use of rTMS in the approved clinical treatment of medication-refractory depression when targeted to the dorsolateral prefrontal cortex (DLPFC), because it is the functional connectivity of the DLPFC to deeper subgenual cingulate cortex that may mediate the mood effects of this stimulation treatment.<sup>54,55</sup>

### **Limitations**

There are a number of limitations, both technical and subject-related, to address. First, there is less experience with TMS-EEG as a measure of cortical physiology than with TMS-MEP, and the use of RMT as the basis for defining stimulation intensities for nonmotor regions of cortex may not be ideal. However, our finding of the augmented late response and its interpretation as a marker of cortical hyperexcitability and persistent activity in epileptic circuits are consistent with the results of other such studies in seizure disorders. There are numerous technical challenges in TMS-EEG data acquisition, including muscle artifact within the first 100 milliseconds poststimulation depending on target location. The effects of this and other sources of artifact were minimized by manual or ICA-based removal. Auditory evoked potential activity related to the clicking sound generated by the TMS coil could be a potential confounding signal that was not removed. However, to contribute to the observed increase in the normalized late

responses, auditory evoked activity would likely have to be systematically diminished in active epilepsy patients relative to controls, as the highest-amplitude activity would be expected to fall within the 100- to 225-millisecond range. We found no differences in raw TMS-evoked potentials between PNH subjects and controls during the relevant time window. Although our study employed only single-pulse stimulation, paired-pulse TMS-EEG is a powerful method of determining hyper- or hypoexcitability within neuronal circuits, and would likely provide useful results in a future study.

It is important to acknowledge our small patient sample. There is clearly interindividual variability in baseline responsiveness to single-pulse stimulation as well as variability within any given individual between different regions of cortex. To address this, we normalized our measures of the late components of the TMS-evoked response as already described. We cannot exclude the possibility that antiepileptic drugs (AEDs) affected our results; all but 1 of our PNH patients were taking AEDs at the time of TMS, and AED usage is known to alter measures of cortical excitability.<sup>56</sup> A subject population free of AEDs or with standardization of medications and serum levels would be ideal, but this was not feasible in our setting. Our findings, however, were robust across subjects, despite variability in the specific AEDs being used, and in general the effect of AEDs is to reduce rather than augment measures of cortical excitability. Finally, PNH is an uncommon disorder, and our findings may have limited applicability to epileptogenesis in the absence of visible anatomical lesions. Further work with a larger population of heterotopia patients will be needed to confirm and extend our results, and similar studies in a broader range of epileptic disorders will be needed to examine whether analogous findings are present in other conditions associated with aberrant cortical connectivity, and to determine whether TMS-EEG metrics are associated with seizure frequency.

### **Conclusions**

As our understanding of epileptogenic mechanisms and markers moves beyond consideration of isolated seizure foci and spontaneous epileptiform discharges, respectively, new methods will be needed to explore pathological circuits and evaluate brain network excitability. Drawing on a small number of patients with a unique developmental form of epilepsy, our work with resting-state functional MRI-guided TMS-EEG demonstrates that such a multimodal methodological approach can be employed to investigate functional cortical changes in central nervous system disease, even when lesions are not apparent or are anatomically remote.

## Acknowledgment

M.M.S. was supported by a KL2/Catalyst Medical Research Investigator Training award from Harvard Catalyst/Harvard Clinical and Translational Science Center (NIH National Center for Research Resources [NCRR] and National Center for Advancing Translational Sciences [NCATS], KL2 TR001100). M.V. was supported by the Fyssen Foundation. C.J.C. was supported by the NIH/NINDS (5K12NS066225). M.B.W. was supported by the American Brain Foundation. A.P.-L. was supported by grants from the Sidney R. Baer Jr Foundation, NIH (NICHD R01 HD069776, NINDS R01 NS073601, NIMH R21 MH099196, NINDS R21 NS082870, NINDS R21 NS085491, NICHD R21 HD07616), and Harvard Catalyst/Harvard Clinical and Translational Science Center (NIH NCRR and the NCATS, UL1 RR025758). B.S.C. was supported by the NIH National Institute of Neurological Disorders and Stroke (R01 NS073601, with subcontract to J.D.E.G.).

The content is solely the responsibility of the authors and does not necessarily represent the official views of Harvard Catalyst, Harvard University and its affiliated academic health care centers, the NIH, or the Sidney R. Baer Jr Foundation.

We thank our subjects, without whom this study could not have been performed; and L. Walker for assistance with subject recruitment.

## Potential Conflicts of Interest

A.P.-L.: grants, Nexstim, Neuronix; scientific advisory boards, Nexstim, Neuronix, Starlab Neuroscience, Neuro-electrics, Neosync; several issued and pending patents on the real-time integration of TMS with EEG and MRI.

## References

- Scharfman HE. The neurobiology of epilepsy. *Curr Neur Neurosci Rep* 2007;7:348–354.
- Spencer SS. Neural networks in human epilepsy: evidence of and implications for treatment. *Epilepsia* 2002;43:219–227.
- Engel J Jr, Thompson PM, Stern JM, et al. Connectomics and epilepsy. *Curr Opin Neurol* 2013;26:186–194.
- Jin X, Prince DA, Huguenard JR. Enhanced excitatory synaptic connectivity in layer V pyramidal neurons of chronically injured epileptogenic neocortex in rats. *J Neurosci* 2006;26:4891–4900.
- Prince DA, Parada I, Scalise K, et al. Epilepsy following cortical injury: cellular and molecular mechanisms as targets for potential prophylaxis. *Epilepsia* 2009;50(suppl 2):30–40.
- Battaglia G, Granata T. Periventricular nodular heterotopia. *Handb Clin Neurol* 2008;87:177–189.
- Aghakhani Y, Kinay D, Gotman J, et al. The role of periventricular nodular heterotopia in epileptogenesis. *Brain* 2005;128:641–651.
- Dubeau F, Tampieri D, Lee N, et al. Periventricular and subcortical nodular heterotopia: a study of 33 patients. *Brain* 1995;118:1273–1287.
- Kothare SV, VanLandingham K, Armon C, et al. Seizure onset from periventricular nodular heterotopias: depth-electrode study. *Neurology* 1998;51:1723–1727.
- Li LM, Dubeau F, Andermann F, et al. Periventricular nodular heterotopia and intractable temporal lobe epilepsy: poor outcome after temporal lobe resection. *Ann Neurol* 1997;41:662–668.
- Tassi L, Colombo N, Cossu M, et al. Electroclinical, MRI and neuropathological study of 10 patients with nodular heterotopia, with surgical outcomes. *Brain* 2005;128:321–337.
- Barkovich AJ, Kjos BO. Gray matter heterotopias: MR characteristics and correlation with developmental and neurologic manifestations. *Radiology* 1992;182:493–499.
- Chang BS, Katzir T, Liu T, et al. A structural basis for reading fluency: white matter defects in a genetic brain malformation. *Neurology* 2007;69:2146–2154.
- Chang BS, Ly J, Appignani B, et al. Reading impairment in the neuronal migration disorder of periventricular nodular heterotopia. *Neurology* 2005;64:799–803.
- Christodoulou JA, Walker LM, Del Tufo SN, et al. Abnormal structural and functional brain connectivity in gray matter heterotopia. *Epilepsia* 2012;53:1024–1032.
- Christodoulou JA, Barnard ME, Del Tufo SN, et al. Integration of gray matter nodules into functional cortical circuits in periventricular heterotopia. *Epilepsy Behav* 2013;29:400–406.
- Archer JS, Abbott DF, Masterton RA, et al. Functional MRI interactions between dysplastic nodules and overlying cortex in periventricular nodular heterotopia. *Epilepsy Behav* 2010;19:631–634.
- Greicius M. Resting-state functional connectivity in neuropsychiatric disorders. *Curr Opin Neurol* 2008;21:424–430.
- Guye M, Bartolomei F, Ranjeva J-P. Imaging structural and functional connectivity: towards a unified definition of human brain organization? *Curr Opin Neurol* 2008;21:393–403.
- Rotenberg A. Prospects for clinical applications of transcranial magnetic stimulation and real-time EEG in epilepsy. *Brain Topogr* 2010;22:257–266.
- Valentin A, Arunachalam R, Mesquita-Rodrigues A, et al. Late EEG responses triggered by transcranial magnetic stimulation (TMS) in the evaluation of focal epilepsy. *Epilepsia* 2008;49:470–480.
- Julkunen P, Saisanen L, Kononen M, et al. TMS-EEG reveals impaired intracortical interactions and coherence in Unverricht-Lundborg type progressive myoclonus epilepsy (EPM1). *Epilepsy Res* 2013;106:103–112.
- Fox MD, Snyder AZ, Vincent JL, et al. The human brain is intrinsically organized into dynamic, anticorrelated functional networks. *Proc Natl Acad Sci U S A* 2005;102:9673–9678.
- Whitfield-Gabrieli S, Thermenos HW, Milanovic S, et al. Hyperactivity and hyperconnectivity of the default network in schizophrenia and in first-degree relatives of persons with schizophrenia. *Proc Natl Acad Sci U S A* 2009;106:1279–1284.
- Behzadi Y, Restom K, Liu J, Liu TT. A component based noise correction method (CompCor) for BOLD and perfusion based fMRI. *Neuroimage* 2007;37:90–101.
- Rorden C, Brett M. Stereotaxic display of brain lesions. *Behav Neurol* 2000;12:191–200.
- Virtanen J, Ruohonen J, Naatanen R, Ilmoniemi RJ. Instrumentation for the measurement of electric brain responses to transcranial magnetic stimulation. *Med Biol Eng Comput* 1999;37:322–326.
- Rossi S, Hallett M, Rossini PM, et al. Safety, ethical considerations, and application guidelines for the use of transcranial magnetic

- stimulation in clinical practice and research. *Clin Neurophysiol* 2009;120:2008–2039.
29. Rossini PM, Barker At, Berardelli A, et al. Non-invasive electrical and magnetic stimulation of the brain, spinal cord, and roots: basic principles and procedures for routine clinical application. Report of an IFCN committee. *Electroencephalogr Clin Neurophysiol* 1994;91:79–92.
  30. Delorme A, Makeig S. EEGLAB: an open source toolbox for analysis of single-trial EEG dynamics including independent component analysis. *J Neurosci Methods* 2004;134:9–21.
  31. Lehmann D, Skrandies W. Reference-free identification of components of checkerboard-evoked multichannel potential fields. *Electroencephalogr Clin Neurophysiol* 1980;48:609–621.
  32. Komssi S, Kahkonen S, Ilmoniemi RJ. The effect of stimulus intensity on brain responses evoked by transcranial magnetic stimulation. *Hum Brain Mapp* 2004;21:154–164.
  33. Kahkonen S, Wilenius J, Komssi S, Ilmoniemi RJ. Distinct differences in cortical reactivity of motor and prefrontal cortices to magnetic stimulation. *Clin Neurophysiol* 2004;115:534–542.
  34. Badawy RA, Curatolo JM, Newton M, et al. Changes in cortical excitability differentiate generalized and focal epilepsy. *Ann Neurol* 2007;61:324–331.
  35. Badawy RA, Macdonell RA, Berkovic SF, et al. Predicting seizure control: cortical excitability and antiepileptic medication. *Ann Neurol* 2010;67:64–73.
  36. Benjamini Y, Hochberg Y. Controlling the false discovery rate: a practical and powerful approach to multiple testing. *J R Stat Soc Series B Stat Methodol* 1995;57:289–300.
  37. Groppe DM, Urbach TP, Kutas M. Mass univariate analysis of event-related brain potentials/fields I: a critical tutorial review. *Psychophysiology* 2011;48:1711–1725.
  38. Hamalainen MS, Sarvas J. Realistic conductivity geometry model of the human head for interpretation of neuromagnetic data. *IEEE Trans Biomed Eng* 1989;36:165–171.
  39. Gramfort A, Luessi M, Larson E, et al. MEG and EEG data analysis with MNE-Python. *Front Neurosci* 2013;7:267.
  40. Fischl B. FreeSurfer. *Neuroimage* 2012;62:774–781.
  41. Kobayashi M, Pascual-Leone A. Transcranial magnetic stimulation in neurology. *Lancet Neurol* 2003;2:145–156.
  42. Hallett M. Transcranial magnetic stimulation: a primer. *Neuron* 2007;55:187–199.
  43. Badawy RA, Vogrin SJ, Lai A, Cook MJ. The cortical excitability profile of temporal lobe epilepsy. *Epilepsia* 2013;54:1942–1949.
  44. Badawy RA, Vogrin SJ, Lai A, Cook MJ. Patterns of cortical hyperexcitability in adolescent/adult-onset generalized epilepsies. *Epilepsia* 2013;54:871–878.
  45. Rogasch NC, Fitzgerald PB. Assessing cortical network properties using TMS-EEG. *Hum Brain Mapp* 2013;34:1652–1669.
  46. Premoli I, Castellanos N, Rivolta D, et al. TMS-EEG signatures of GABAergic neurotransmission in the human cortex. *J Neurosci* 2014;34:5603–5612.
  47. Li H, McDonald W, Parada I, et al. Targets for preventing epilepsy following cortical injury. *Neurosci Lett* 2011;497:172–176.
  48. Bladin CF, Bornstein N. Post-stroke seizures. *Handb Clin Neurol* 2009;93:613–621.
  49. Bonilha L, Nesland T, Martz GU, et al. Medial temporal lobe epilepsy is associated with neuronal fibre loss and paradoxical increase in structural connectivity of limbic structures. *J Neurol Neurosurg Psychiatry* 2012;83:903–909.
  50. Fox MD, Greicius M. Clinical applications of resting state functional connectivity. *Front Syst Neurosci* 2010;4:19.
  51. Fregni F, Otachi PTM, do Valle A, et al. A randomized clinical trial of repetitive transcranial magnetic stimulation in patients with refractory epilepsy. *Ann Neurol* 2006;60:447–455.
  52. Sun W, Mao W, Meng X, et al. Low-frequency repetitive transcranial magnetic stimulation for the treatment of refractory partial epilepsy: a controlled clinical study. *Epilepsia* 2012;53:1782–1789.
  53. Wagner T, Gangitano M, Romero R, et al. Intracranial measurement of current densities induced by transcranial magnetic stimulation in the human brain. *Neurosci Lett* 2004;354:91–94.
  54. Fox MD, Buckner RL, White MP, et al. Efficacy of transcranial magnetic stimulation targets for depression is related to intrinsic functional connectivity with the subgenual cingulate. *Biol Psychiatry* 2012;72:595–603.
  55. Downar J, Daskalakis ZJ. New targets for rTMS in depression: a review of convergent evidence. *Brain Stim* 2013;6:231–240.
  56. Badawy RA, Macdonell RA, Berkovic SF, et al. Predicting seizure control: cortical excitability and antiepileptic medication. *Ann Neurol* 2010;67:64–73.